ChemComm

COMMUNICATION

View Article Online
View Journal | View Issue

Cite this: *Chem. Commun.*, 2017, 53, 8529

Received 8th May 2017,
Accepted 7th July 2017

DOI: 10.1039/c7cc03572a

rsc.li/chemcomm

Evaluation of DFO-HOPO as an octadentate chelator for zirconium-89†

L. Allott, ‡[a] C. Da Pieve,‡[a] J. Meyers,[b] T. Spinks,[a] D. M. Ciobota,[a] G. Kramer-Marek[a] and G. Smith *[a]

The future of ^{89}Zr-based immuno-PET is reliant upon the development of new chelators with improved stability compared to the currently used deferoxamine (DFO). Herein, we report the evaluation of the octadentate molecule DFO-HOPO (3) as a suitable chelator for ^{89}Zr and a more stable alternative to DFO. The molecule showed good potential for the future development of a DFO-HOPO-based bifunctional chelator (BFC) for the radiolabelling of biomolecules with ^{89}Zr. This work broadens the selection of available chelators for ^{89}Zr in search of improved successors to DFO for clinical ^{89}Zr-immuno-PET.

An increasing interest in zirconium-89 (^{89}Zr) for preclinical and clinical immuno-positron emission tomography (immuno-PET) is due to its favourable decay characteristics ($t_{1/2}$ = 78.4 h, β^+ = 22.8%, $E_{\beta+\max}$ = 901 keV) for the radiolabelling of antibodies which have long biological half-lives.[1–4] Currently, deferoxamine (DFO) is the chelator most commonly used to radiolabel biomolecules with ^{89}Zr.[5] DFT modelling showed that the coordination sphere in the Zr–DFO complex consists of the Zr^{4+} cation, six donor atoms belonging to the DFO molecule, and two other coordination sites being occupied by water molecules.[6,7] As a result of this incomplete coordination of ^{89}Zr by the hexadentate DFO molecule, the ^{89}Zr–DFO complex undergoes a certain degree of demetallation *in vivo* with the released ^{89}Zr taken up by the bone.[8] This is of concern because bone uptake of free $^{89}Zr^{4+}$ is undesirable owing to the high radiation dose to bone marrow; furthermore this background uptake can confound image acquisition of bone malignancies such as bone metastases. To solve the instability, different strategies have been investigated. Alternative hexadentate macrocycles (*i.e.* Fusarinine C) and hydroxypyridinone-based compounds (*i.e.* CP256) have been produced and tested but showed either no improvement or reduced stability *in vivo* when compared to DFO.[9,10] Additionally, a variety of either linear or macrocyclic octadentate chelators have been developed with structures hinged around hydroxamic acid or hydroxypyridinone moieties which resulted in ^{89}Zr-complexes displaying either increased or decreased stability compared to DFO.[11–19] White *et al.* described the use of a DFO-1-hydroxy-2-pyridone ligand (DFO-HOPO) as an effective sequestering agent for the treatment of plutonium(IV) poisoning (Fig. 1).[20] The authors showed that the addition of one 1,2-HOPO molecule to DFO produced a low toxicity octadentate chelator which yielded very stable complexes with Pu(IV) at physiological pH. Herein, we report an updated synthesis of DFO-HOPO (3) which was then evaluated as an octahedral ligand for ^{89}Zr. The stability of the radiocomplex was tested *in vitro* and *in vivo* and compared to ^{89}Zr–DFO in order to confirm 3 as a viable alternative to the chelators for ^{89}Zr already described in the literature.

The synthesis of DFO-HOPO (3) was adapted from a literature procedure.[20] In brief, commercially available DFO was reacted with hydroxamic acid chloride (2) and the product (3) was isolated by semi-preparative RP-HPLC (Scheme S1, ESI†). No protection of the *N*-hydroxyl group of 1 was necessary. To determine and characterise the coordination capabilities of the chelator, the

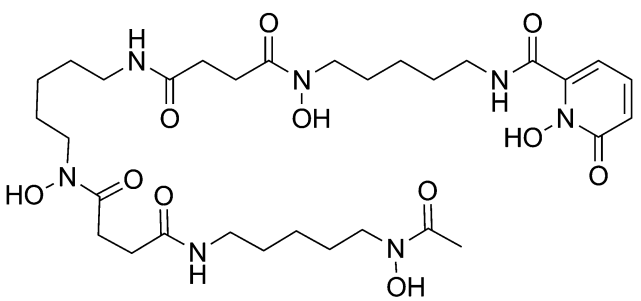

3

Fig. 1 Structure of DFO-HOFO (3) containing three hydroxamic acid and one hydroxypyridone moiety for coordinating $^{89}Zr^{4+}$.

[a] *Division of Radiotherapy and Imaging, The Institute of Cancer Research, 123 Old Brompton Road, London, UK. E-mail: graham.smith@icr.ac.uk*
[b] *Cancer Research UK Cancer Therapeutics Unit, Division of Cancer Therapeutics, The Institute of Cancer Research, 123 Old Brompton Road, London, UK*

† Electronic supplementary information (ESI) available: Materials and methods, NMR, HRMS and HPLC data, DFT calculations, radiolabelling and stability studies, *in vivo* data. See DOI: 10.1039/c7cc03572a

‡ Author contributions: equal contribution for first authorship.

non-radioactive ^{nat}Zr complex of DFO-HOPO (^{nat}Zr-**3**) was prepared in macroscopic scale by mixing the chelator with $ZrCl_4$ at room temperature. Showing the value of 784.247 *m/z*, the high resolution mass spectrometry (HRMS) analysis of ^{nat}Zr-**3** confirmed the expected complex mass to indicate a metal-to-ligand binding ratio of 1 : 1. Examination by RP-HPLC showed the elution of ^{nat}Zr-**3** as a single peak at 7 : 20 (min : s), *ca.* 33 seconds before HOPO-DFO (**3**). The coordination of the metal ion by the chelator was further confirmed by infrared spectroscopy (IR) analysis which showed a red-shift in the main carbonyl stretching band from *ca.* 1620 to *ca.* 1600 cm^{-1}. Additional characterisation of the complex by ultraviolet-visible spectroscopy (UV-Vis) showed no detectable difference between the absorption spectra of ^{nat}Zr-**3** and **3**. Moreover, NMR analysis of the ^{nat}Zr complex could not be performed due to its poor solubility in any solvent, which is expected to be resolved upon bioconjugation.

To verify the steric and electronic ability of **3** to form a Zr(IV) octadentate chelate, density functional theory (DFT) calculations were carried out. The optimised geometry (based on the lower energy conformation) shows the metal centre coordinated to eight oxygen atoms of the chelator (Fig. 2). The Zr–O bond distances were in the range of 2.14–2.36 Å, in agreement with values reported in the literature for similar complexes.[11,12]

The preparation of ^{89}Zr-**3** was performed as previously described in the literature for ^{89}Zr–DFO.[21] Incubating the chelator with a neutralised ^{89}Zr solution at room temperature for 1 h (pH 7) guaranteed a quantitative (>99%) radiolabelling up to a specific activity of 20 MBq $nmol^{-1}$ even at low concentration of the chelator (3–8 μM). A comparable radiolabelling efficiency was obtained for ^{89}Zr–DFO. All reactions were monitored by radio-active instant thin layer chromatography (radio-ITLC). A variety of mobile and stationary phases were tested to find the optimum analytical conditions for both ^{89}Zr-**3** and ^{89}Zr–DFO, which was used as a comparison. The elution profiles of both the radioactive complexes were affected by the type of stationary phase employed, and only the positively charged ^{89}Zr–DFO (consequence of the hexadentate chelation of ^{89}Zr) was influenced also by the mobile phase pH, when SG-ITLC strips were used. The results suggest that, differently from ^{89}Zr–DFO, ^{89}Zr-**3** is present in solution as a neutral complex, achievable through the octadentate chelation of ^{89}Zr. This finding further advocates the involvement of the 1,2-HOPO moiety of **3** in the coordination of the metal centre. Enabling the elution of ^{89}Zr-**3** and the ^{89}Zr–DFO as well defined and separated bands (R_f of 0.6 and 0.1 respectively on SG-ITLC strips), ammonium acetate (0.1 M, pH 7) was used as mobile phase for the ITLC analysis. Interestingly, the radio-ITLC of ^{89}Zr-**3** revealed the presence of two well-separated spots (R_f of *ca.* 0.6 and 0.1); the relative intensity of the spots was dependent on the specific activity of the product (*i.e.* concentration of the chelator) and on time. By lowering the specific activities of the product, with a consequent increase of the concentration of **3**, a decrease of the band having R_f = 0.1 was observed. After 24 hours at ambient temperature, only the band having R_f = 0.6 was detected. To probe the influence of temperature on the formation of the two products, the radiolabelling reaction was performed at 80 °C. Although the quantity of product eluting with an R_f = 0.1 was reduced, the increased temperature did not prevent it from forming. These observations suggest that the two bands represent two different forms of the ^{89}Zr-**3** complex; an initial transitional kinetic product which converted into a final thermodynamically stable product. Examination of the chromatographic data of ^{89}Zr-**3** could help explain the phenomenon; the transitional product was detected at the origin of the radio-ITLC strip (R_f = 0.1 at pH 7) suggesting it was charged (similarly to hexacoordinated ^{89}Zr–DFO), possibly as the result of incomplete coordination of the radiometal. With an R_f = 0.6 (at pH 7), the thermo-dynamically stable final product was most likely neutral, a condition which would be achieved by the complete chelation of ^{89}Zr by octadentate **3**. Moreover, radio-HPLC analysis of ^{89}Zr-**3** after 24 hours showed only one product (corresponding to the band with R_f = 0.6 on radio-ITLC) having an elution profile very similar to that of ^{nat}Zr-**3** suggesting a similar identity as an octadentate complex. Importantly, no ^{89}Zr was released during the transition.

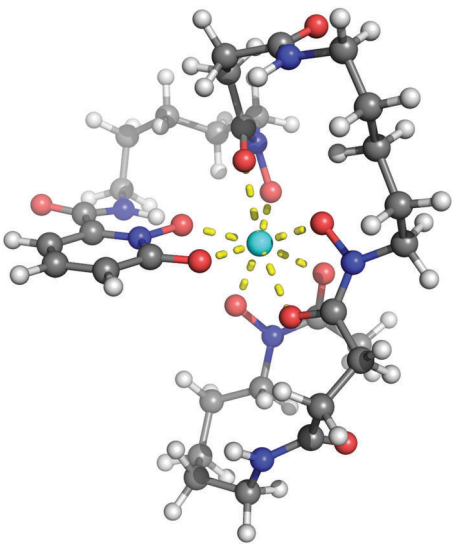

Fig. 2 The DFT optimised structure of ^{89}Zr-**3**. (Atom colour: white = hydrogen; grey = carbon; blue = nitrogen; red = oxygen; cyan = zirconium.)

The stability of ^{89}Zr-**3** was initially assessed by a simple radio-ITLC analysis using an acidic buffer (pH 2) as mobile phase. Differently from ^{89}Zr–DFO (14.4 ± 4.65% radioactivity not associated with DFO), ^{89}Zr-**3** showed no demetallation as a result of the enhanced coordination of the metal centre by the octadentate ligand. To mimic what might happen *in vivo*, a challenge assay assessed the stability of ^{89}Zr-**3** to transchelation in the presence of a large excess of either EDTA or DFO (pH 7). In both challenges, ^{89}Zr-**3** showed no transchelation with >99% intact complex after 7 days (Table 1). By comparison, ^{89}Zr–DFO demonstrated transchelation toward EDTA with 65.5% of intact complex after 7 days (Table 1). Moreover, a complete trans-metallation of ^{89}Zr–DFO towards **3** was achieved in a matter of hours. Further experiments aiming to test the inertness of ^{89}Zr-**3** were performed in mouse serum. With >99% intact complex after incubation at 37 °C for 7 days, ^{89}Zr-**3** showed a higher stability compared to ^{89}Zr–DFO (90.6% intact complex) (Table 1).

Table 1 The stability of ^{89}Zr-**3** and ^{89}Zr–DFO was tested against transchelation in the presence of an excess of competitor chelator over seven days (pH 7). The controls (complexes in solution without competitor) show high stability (>99% intact complex) (**A**). The stability of the ^{89}Zr-complexes was also tested in mouse serum over seven days (**B**). All experiments were performed in triplicate

			Fraction of intact complex (% ±SD)					
	Complex	Competitor	0 min	1 h	3 h	1 d	3 d	7 d
A	^{89}Zr-**3**	EDTA	>99	>99	>99	>99	>99	>99
		DFO	>99	>99	>99	>99	>99	>99
	^{89}Zr–DFO	EDTA	>99	>99	>99	75.63 ± 3.07	63.1 ± 0.75	65.5 ± 4.42
		3	>99	35.8 ± 9.8	4.1 ± 2.35	0	0	0
B	^{89}Zr-**3**	Mouse serum	>99	—	>99	>99	>99	>99
	^{89}Zr–DFO	Mouse serum	>99	—	>99	97.7 ± 0.53	94.7 ± 0.78	90.6 ± 1.75

PET imaging and comparative biodistribution studies were performed in healthy mice for ^{89}Zr-**3** and ^{89}Zr–DFO. At 1 h p.i. of ^{89}Zr-**3**, the radioactivity was observed mainly in the bladder and intestine; some activity was also visible in the gall bladder. At 4 and 24 h p.i., most of the residual radioactivity was in the gut. These observations indicate a rapid renal clearance together with slower hepatobiliary excretion. The hydrophilicity of the complexes is an important physiochemical property which regulates their distribution, metabolism, and elimination *in vivo*. The $\log D_{7.4}$ of neutral complex ^{89}Zr-**3** was found to be −0.87 ± 0.03 which indicates a less hydrophilic character than the positively charged ^{89}Zr–DFO (−3.0 ± 0.01) and can explain the clearance pathway.[9] After 24 h, the radioactivity level was minimal therefore no additional imaging studies at longer time points were carried out. Importantly, no uptake of ^{89}Zr in the bone was observed at any time point (Fig. 3).

Corroborating the PET images, the biodistribution studies clearly showed the participation of both the renal and hepatobiliary systems in the clearance of ^{89}Zr-**3** (Fig. 4). Most of the radioactivity had already cleared through the kidneys at 1 h p.i. (1.39 ± 0.1% ID per g), while at 4 h p.i. the residual activity was localised in the gut (mostly small intestine with 0.898 ± 0.252% ID per g). Differently from ^{89}Zr–DFO (0.93 ± 0.11% ID per g still present in the kidneys), ^{89}Zr-**3** was almost completely cleared from the body at 24 h p.i. Although the values are quite low, ^{89}Zr–DFO showed *ca.* 10-fold higher activity accumulation in the bone than ^{89}Zr-**3** at 24 h p.i. (0.037 ± 0.002 and 0.004 ± 0.001 for ^{89}Zr–DFO and ^{89}Zr-**3** respectively). This phenomenon could be correlated to either the higher level of radioactivity still present in the animals injected with ^{89}Zr–DFO or to an improved *in vivo* stability of ^{89}Zr-**3** compared to ^{89}Zr–DFO.

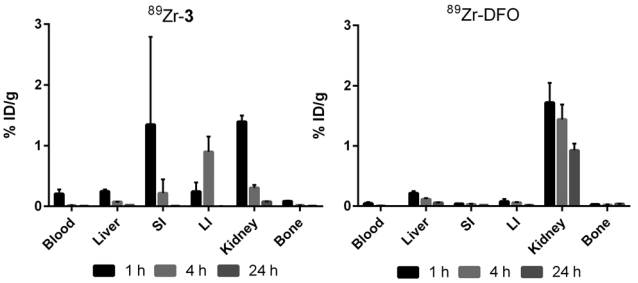

Fig. 4 Biodistribution data for ^{89}Zr-**3** and ^{89}Zr–DFO at 1, 4 and 24 h p.i. in selected organs. SI = small intestine; LI = large intestine. All experiments were performed in triplicate.

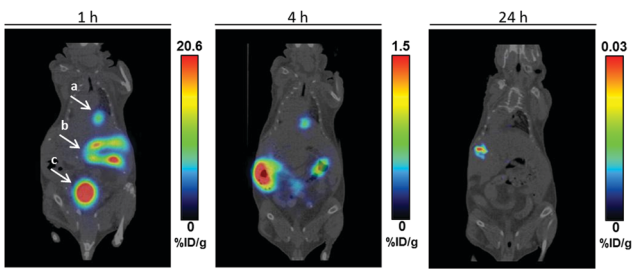

Fig. 3 Coronal PET images of ^{89}Zr-**3** in a healthy mouse at 1, 4 and 24 h p.i. The white arrows indicate the gall bladder (a), intestine (b) and the bladder (c). An almost complete clearance of ^{89}Zr-**3** was observed after 24 h.

In summary, the ^{89}Zr-**3** complex exhibited improved stability compared to ^{89}Zr–DFO in both challenge assays and in serum; the capability and favourability of **3** to form a stable chelate was clearly demonstrated by the complete transchelation of ^{89}Zr from ^{89}Zr–DFO in *ca.* 3 h. The *in vivo* studies showed that ^{89}Zr-**3** cleared the body *via* the renal and hepatobiliary systems. However, once conjugated to a biomolecule the pharmacokinetics of the final radioconjugate will depend mainly on the biomolecule itself. Importantly, the straightforward synthesis of **3** from the commercially available DFO is amenable to allow the synthesis of a bifunctional chelator which is currently underway in our laboratory. This could be achieved by using a similar strategy described by Patra *et al.* for the synthesis of DFO*, where a molecule (or a variety of molecules) containing both the bidentate moiety and a reactive functionality for bioconjugation is attached to the free amine of DFO.[11] The promising DFO-HOPO molecule is a valuable addition to the selection of available chelators for ^{89}Zr in search of successful successors of DFO for clinical immuno-PET applications based on important characteristics such as synthesis, chelate stability and *in vivo* pharmacokinetics.

We thank Tom Burley and Steven Turnock for valuable technical help. This work was supported by the Cancer Research UK – Cancer Imaging Centre (grant ref: C1060/A16464) and Wellcome Trust grant 102361/Z/13/Z. This report is independent research funded by the National Institute for Health Research. The views expressed in this publication are those of the authors

and not necessarily those of the NHS, the National Institute for Health Research or the Department of Health.

Notes and references

1 M. A. Deri, B. M. Zeglis, L. C. Francesconi and J. S. Lewis, *Nucl. Med. Biol.*, 2013, **40**, 3–14.
2 G. Fischer, U. Seibold, R. Schirrmacher, B. Wängler and C. Wängler, *Molecules*, 2013, **18**, 6469–6490.
3 Y. W. S. Jauw, C. W. Menke-vander Houven van Oordt, O. S. Hoekstra, N. H. Hendrikse, D. J. Vugts, J. M. Zijlstra, M. C. Huisman and G. A. van Dongen, *Front. Pharmacol.*, 2016, **7**, DOI: 10.3389/fphar.2016.00131.
4 D. J. Vugts, G. W. M. Visser and G. A. M. S. v. Dongen, *Curr. Top. Med. Chem.*, 2013, **13**, 446–457.
5 G. W. Severin, J. W. Engle, R. J. Nickles and T. E. Barnhart, *Med. Chem.*, 2011, **7**, 389–394.
6 J. P. Holland, V. Divilov, N. H. Bander, P. M. Smith-Jones, S. M. Larson and J. S. Lewis, *J. Nucl. Med.*, 2010, **51**, 1293–1300.
7 J. P. Holland and N. Vasdev, *Dalton Trans.*, 2014, **43**, 9872–9884.
8 J. P. Holland, V. Divilov, N. H. Bander, P. M. Smith-Jones, S. M. Larson and J. S. Lewis, *J. Nucl. Med.*, 2010, **51**, 1293–1300.
9 C. Zhai, D. Summer, C. Rangger, G. M. Franssen, P. Laverman, H. Haas, M. Petrik, R. Haubner and C. Decristoforo, *Mol. Pharmaceutics*, 2015, **12**, 2142–2150.
10 M. T. Ma, L. K. Meszaros, B. M. Paterson, D. J. Berry, M. S. Cooper, Y. Ma, R. C. Hiderd and P. J. Blower, *Dalton Trans.*, 2015, **44**, 4884–4900.
11 M. Patra, A. Bauman, C. Mari, C. A. Fischer, O. Blacque, D. Häussinger, G. Gasser and T. L. Mindt, *Chem. Commun.*, 2014, **50**, 11523–11525.
12 M. A. Deri, S. Ponnala, B. M. Zeglis, G. Pohl, J. J. Dannenberg, J. S. Lewis and L. C. Francesconi, *J. Med. Chem.*, 2014, **57**, 4849–4860.
13 F. Guérard, Y.-S. Lee and M. W. Brechbiel, *Chem. – Eur. J.*, 2014, **20**, 5584–5591.
14 D. N. Pandya, S. Pailloux, D. Tatum, D. Magda and T. J. Wadas, *Chem. Commun.*, 2015, **51**, 2301–2303.
15 S. E. Rudd, P. Roselt, C. Cullinane, R. J. Hicks and P. S. Donnelly, *Chem. Commun.*, 2016, **52**, 11889–11892.
16 J. Rousseau, Z. Zhang, G. M. Dias, C. Zhang, N. Colpo, F. Bénard and K.-S. Lin, *Bioorg. Med. Chem. Lett.*, 2017, **27**, 734–738.
17 E. Boros, J. P. Holland, N. Kenton, N. Rotile and P. Caravan, *ChemPlusChem*, 2016, **81**, 274–281.
18 D. J. Vugts, C. Klaver, C. Sewing, A. J. Poot, K. Adamzek, S. Huegli, C. Mari, G. W. Visser, I. E. Valverde, G. Gasser, T. L. Mindt and G. A. van Dongen, *Eur. J. Nucl. Med. Mol. Imaging*, 2017, **44**, 286–295.
19 D. N. Pandya, N. Bhatt, H. Yuan, C. S. Day, B. M. Ehrmann, M. Wright, U. Bierbach and T. J. Wadas, *Chem. Sci.*, 2017, **8**, 2309–2314.
20 D. L. White, P. W. Durbin, N. Jeung and K. N. Raymond, *J. Med. Chem.*, 1988, **31**, 11–18.
21 M. J. W. D. Vosjan, L. R. Perk, G. W. M. Visser, M. Budde, P. Jurek, G. E. Kiefer and G. A. M. S. v. Dongen, *Nat. Protoc.*, 2010, **5**, 739–743.

